9-23-2015

Evidence for differential viral oncolytic efficacy in an in vitro model of epithelial ovarian cancer metastasis

Jessica G. Tong
Western University

Yudith R. Valdes
London Regional Cancer Program

John W. Barrett
London Regional Cancer Program

John C. Bell
University of Ottawa

David Stojdl
University of Ottawa

See next page for additional authors

Authors
Jessica G. Tong, Yudith R. Valdes, John W. Barrett, John C. Bell, David Stojdl, Grant McFadden, J. Andrea McCart, Gabriel E. DiMattia, and Trevor G. Shepherd

Citation: Molecular Therapy — Oncolytics (2015) **2,** 15013; doi:10.1038/mto.2015.13
Official journal of the American Society of Gene & Cell Therapy

www.nature.com/mto

ARTICLE

Evidence for differential viral oncolytic efficacy in an *in vitro* model of epithelial ovarian cancer metastasis

Jessica G Tong[1,2], Yudith Ramos Valdes[1], John W Barrett[3], John C Bell[4,5], David Stojdl[6], Grant McFadden[7], J Andrea McCart[8], Gabriel E DiMattia[1,9,10,11] and Trevor G Shepherd[1,2,10,11]

Epithelial ovarian cancer is unique among most carcinomas in that metastasis occurs by direct dissemination of malignant cells traversing throughout the intraperitoneal fluid. Accordingly, we test new therapeutic strategies using an *in vitro* three-dimensional spheroid suspension culture model that mimics key steps of this metastatic process. In the present study, we sought to uncover the differential oncolytic efficacy among three different viruses—Myxoma virus, double-deleted vaccinia virus, and Maraba virus—using three ovarian cancer cell lines in our metastasis model system. Herein, we demonstrate that Maraba virus effectively infects, replicates, and kills epithelial ovarian cancer (EOC) cells in proliferating adherent cells and with slightly slower kinetics in tumor spheroids. Myxoma virus and vaccinia viruses infect and kill adherent cells to a much lesser extent than Maraba virus, and their oncolytic potential is almost completely attenuated in spheroids. Myxoma virus and vaccinia are able to infect and spread throughout spheroids, but are blocked in the final stages of the lytic cycle, and oncolytic-mediated cell killing is reactivated upon spheroid reattachment. Alternatively, Maraba virus has a remarkably reduced ability to initially enter spheroid cells, yet rapidly infects and spreads throughout spheroids generating significant cell killing effects. We show that low-density lipoprotein receptor expression in ovarian cancer spheroids is reduced and this controls efficient Maraba virus binding and entry into infected cells. Taken together, these results are the first to implicate the potential impact of differential viral oncolytic properties at key steps of ovarian cancer metastasis.

Molecular Therapy — Oncolytics (2015) **2**, 15013; doi:10.1038/mto.2015.13; published online 23 September 2015

INTRODUCTION

Epithelial ovarian cancer (EOC) is the most lethal gynecologic malignancy and represents the sixth most commonly diagnosed cancer among women in the developed world.[1] A lack of effective therapeutic options, coupled with the highly heterogeneous nature of EOC, and being typically diagnosed at an advanced metastatic stage, contribute to the lethality of EOC.[2,3] Current therapeutic strategies involve exhaustive cytoreductive surgery and postoperative platinum- and taxane-based chemotherapy.[4–6] However, effective treatment is complicated by the manifestation of EOC as multiple histotypes, which are differentially responsive to platinum- and taxane-based combination chemotherapy treatments.[7] Furthermore, patients that initially respond well to platinum therapy almost inevitably relapse with chemo-resistant disease resulting in reduced overall survival. Thus, there is a critical need for targeted and durable therapeutic alternatives beyond the standard first-line chemotherapeutic agents.[8–10]

Oncolytic virotherapy promotes selective viral infection and lysing of cancer cells. The specific nature of oncolytic virus therapy stems from the selection of non- or low-pathogenic nonhuman viruses that display tropism for cancer-associated genetic mutations or aberrant signaling.[11] Myxoma virus (MYXV) is a European rabbit-specific poxvirus that has not been shown to cause disease in humans and is used as a pesticide to control Australian rabbit populations.[12] MYXV displays tropism for cancer cells with upregulation in active AKT signaling and dysfunctional p53, which is found in essentially all high-grade EOC.[13] Conversely, vvDD is an engineered poxvirus with deleted vaccinia growth factor and viral thymidine kinase genes, which limit its infection to cells harboring upregulated EGFR/RAS signaling commonly observed in low-grade EOCs.[14] Point mutations in the strain of MRBV used in this study modify the matrix protein (M) and glycoprotein (G) effectively boosting its replicative capacity in cancer cells while rendering it unable to counteract an antiviral type I interferon response in healthy cells. Though its specific tropism for cancer cells is relatively undefined, MRBV has been shown to have potent oncolytic effects in a broad range of cancer cells, including EOC.[15]

The mode of EOC metastasis is unique among most solid malignancies, and therefore it likely possesses distinct and novel mechanisms. EOC metastasis occurs via the shedding of malignant cells from the primary tumor into the peritoneal cavity; this

[1]Translational Ovarian Cancer Research Program, London Regional Cancer Program, London, Ontario, Canada; [2]Department of Anatomy & Cell Biology, Western University, London, Ontario, Canada; [3]Translational Head and Neck Cancer Research Program, London Regional Cancer Program, London, Ontario, Canada; [4]Department of Medicine & Biochemistry, University of Ottawa, Ottawa, Ontario, Canada; [5]Department of Microbiology and Immunology, University of Ottawa, Ottawa, Ontario, Canada; [6]Department of Pediatrics, University of Ottawa, Ottawa, Ontario, Canada; [7]Department of Molecular Genetics & Microbiology, University of Florida, Gainesville, Florida, USA; [8]Department of Surgery, University of Toronto, Toronto, Ontario, Canada; [9]Department of Biochemistry, Western University, London, Ontario, Canada; [10]Department of Oncology, Western University, London, Ontario, Canada; [11]Department of Obstetrics & Gynaecology, Western University, London, Ontario, Canada. Correspondence: TG Shepherd (tshephe6@uwo.ca)
Received 16 April 2015; accepted 6 July 2015

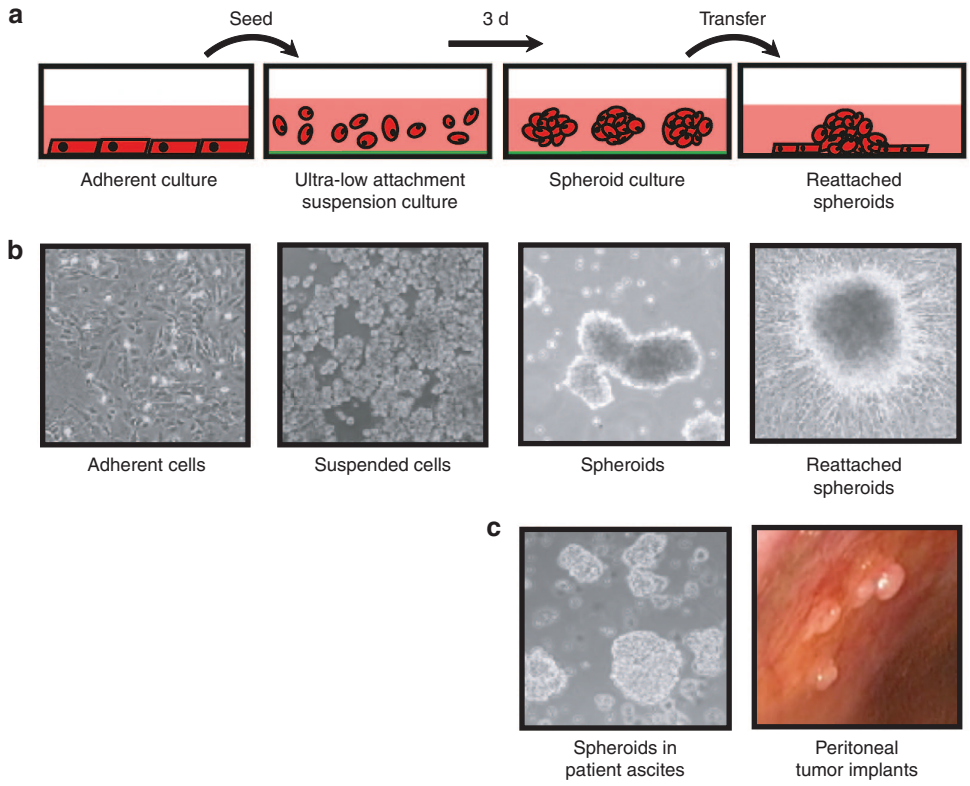

Figure 1 *In vitro* three-dimensional spheroid model system of ovarian cancer metastasis. (**a**) Ovarian cancer cells are grown as adherent proliferating monolayer cultures, and are transferred to Ultra-Low Attachment tissue culture plastic-ware where they naturally form multicellular aggregates, or spheroids, when in suspension culture. Spheroids are subsequently transferred back to standard tissue culture plastic to facilitate adhesion and growth of cells out of viable spheroids. (**b**) Phase contrast images of ovarian cancer cells in each of the culture conditions outlined in panel **a**. (**c**) Left: Phase contrast microscopic image of freshly-collected ovarian cancer patient ascites indicating the presence of spheroids in suspension. Right: Image representing ovarian tumor nodules implanted on the peritoneal wall of an ovarian cancer patient at the time of laparoscopic surgery.

can occur in the context of ascites, an exudative fluid commonly associated with advanced-stage disease. Single cells in suspension within the ascites are susceptible to death through anoikis; thus aggregation of single cells into multicellular spheroids facilitates escape from cell death.[16,17] Furthermore, EOC spheroid survival is maintained in the low-nutrient environment of the ascites by undergoing cellular quiescence and autophagy.[18,19] This tumor cell dormancy phenotype within spheroids is thought to allow persistence of microscopic EOC secondary deposits after treatment with first-line chemotherapeutics and support growth under more favorable conditions.[20] In addition, spheroids have an enhanced capacity to attach and invade mesothelial-lined surfaces in the peritoneal space promoting the formation of secondary tumor nodules.[16]

We postulate that in the context of metastatic ovarian cancer, the ability to kill dormant tumor cells is essential to eradicate the potential for disease recurrence. In this study, we compare three oncolytic viruses, MYXV, vvDD and MRBV, in an *in vitro* spheroid culture model of ovarian cancer metastasis to determine whether they have the potential to kill dormant tumor cells residing in spheroids.

RESULTS

Oncolytic effects of MYXV, vvDD, and MRBV in ovarian cancer cell lines

To begin to define the optimal oncolytic viral approach to the eradication of dormant EOC cells in spheroids, we applied three different viruses in an *in vitro* three-dimensional spheroid culture system, which we have established to model metastatic EOC (Figure 1). Distinct molecular characteristics typify the lifecycle of metastatic ovarian cancer cells as they move from a proliferative state in the solid tumor to the resting state in ascites-suspended spheroids and finally when these structures attach to a secondary site and cells proliferate to form a metastatic lesion. Herein, we performed oncolytic infections using proliferating adherent EOC cell lines, spheroids cultured in suspension, and spheroid reattachment to tissue culture substratum to determine whether molecular and cellular changes at these specific steps would affect oncolytic virus cell killing efficacy. We selected the established HEYA8, SKOV3 and OVCAR8 cell lines since they have been well-characterized genomically (Supplementary Table S1) and have been predicted to represent different EOC subtypes based on this data.[21]

First, we performed parallel viral infections of adherent EOC cell lines with established spheroids in suspension (Figure 2a). Even in proliferating adherent cultures, we found that MYXV, vvDD, and MRBV were capable of inducing oncolysis of EOC lines with differential killing capacities among the three viruses and across cell lines (Figure 2). MYXV displayed the least potent killing and was unable to induce significant oncolysis at less than a multiplicity of infection (MOI) 1 in all cell lines (Figure 2b). vvDD exhibited oncolysis at similar concentrations as MYXV, but was able to induce greater loss of viability in comparison. Among the three EOC cell lines, OVCAR8 cells displayed greatest sensitivity to vvDD and MYXV infection whereas SKOV3 cells were most resistant in adherent culture infections. In a similar fashion, when tested using ovarian cancer patient ascites-derived primary cultures, vvDD yielded better oncolytic activity than MYXV in the majority of clinical samples (Supplementary Figure S1). Although both MYXV and vvDD were

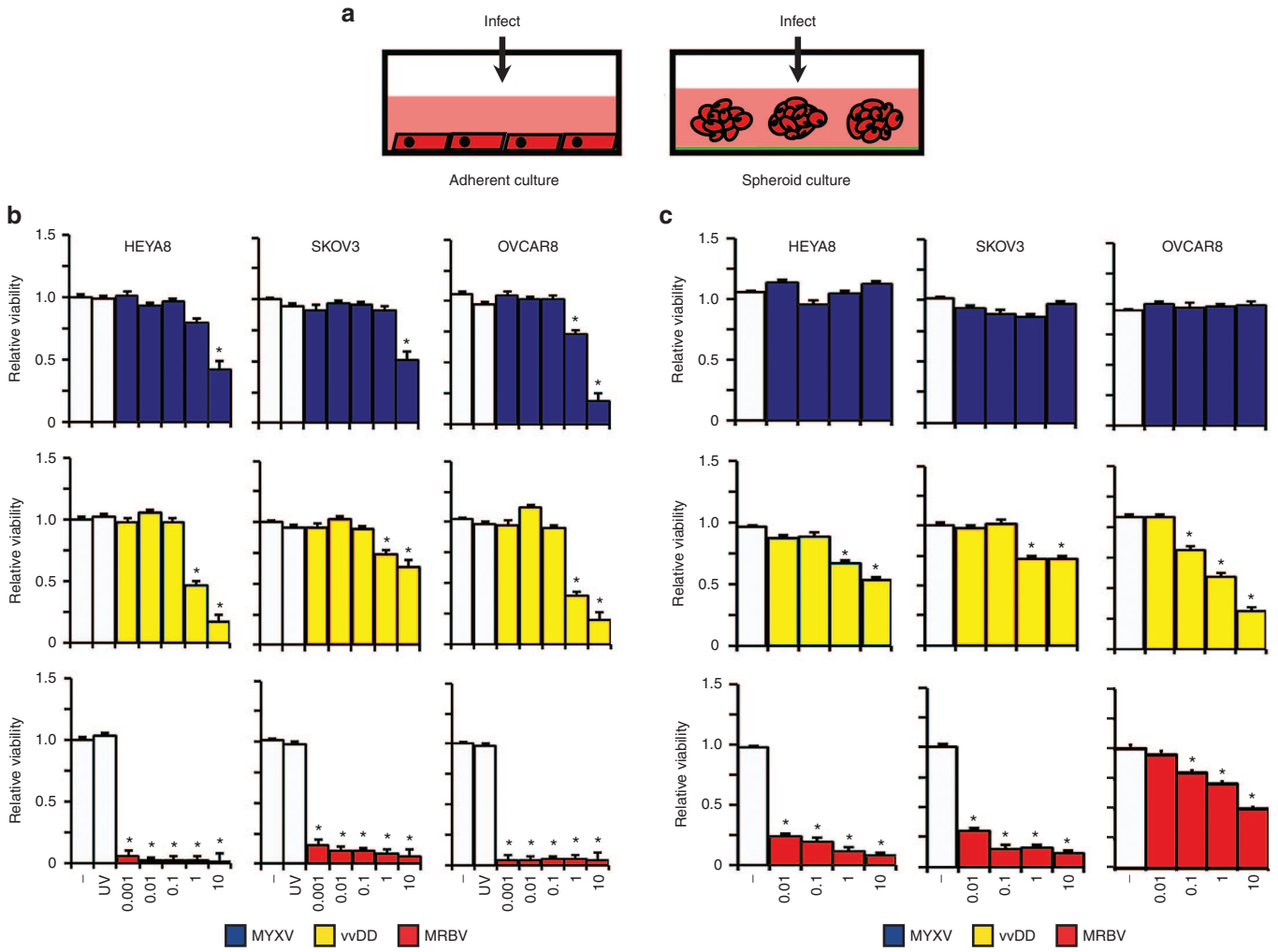

Figure 2 Analysis of MYXV, vvDD, and MRBV oncolytic-mediated killing of EOC cell lines in adherent and spheroid culture. (**a**) Schematic representation of viral infection of ovarian cancer cells in adherent and spheroid culture. (**b**) HEYA8, SKOV3, and OVCAR8 cells were infected at increasing concentrations to a maximum of multiplicity of infection (MOI) 10, as indicated; UV-inactivated virus was used at a MOI of 10. Cell viability was measured after 72 hours using CellTiter-Glo. (**c**) HEYA8, SKOV3, and OVCAR8 cells were seeded to Ultra-Low Attachment dishes to form spheroids over 3 days, then infected at the indicated doses; spheroid cell viability was assayed as in panel **b** (*$P < 0.05$). EOC, epithelial ovarian cancer; MYXV, Myxoma virus.

able to induce modest oncolysis of EOC cell lines in adherent culture, infection-mediated cell killing was dramatically reduced in EOC spheroids for all cell lines tested (Figure 2c). vvDD was completely ineffective at inducing oncolysis of SKOV3 spheroids, but it did maintain some oncolytic activity in HEYA8 and OVCAR8 spheroids.

These findings using MYXV and vvDD were in stark contrast to results of MRBV infection, which induced robust oncolysis-mediated cell killing across all EOC cell lines in adherent culture even at an MOI of 0.001 (Figure 2b). In contrast, MRBV infection of heterogeneous patient-derived cells yielded highly variable oncolytic effects with one sample exhibiting robust MRBV-mediated loss in cell viability similar to established EOC cell lines (Supplementary Figure S1). However, a potent oncolytic effect was observed in MRBV-infected HEYA8 and SKOV3 spheroids where dramatic loss of cellular viability was evident with as little as MOI 0.01 at three days postinfection. Interestingly, we observed a significant reduction in MRBV oncolytic effects in OVCAR8 spheroids compared with adherent cells suggesting that EOC cells may have the capacity to acquire resistance against MRBV infection in three-dimensional spheroid form (Figure 2c).

MRBV is significantly faster at inducing oncolysis of EOC cells

We hypothesized that the potent oncolysis of EOC cells by MRBV may be due to a rapid ability to replicate its small RNA-based genome, allowing it to complete multiple rounds of infection within the experimental time frame of 72 hours. MRBV contrasts the large poxviruses, MYXV and vvDD, which have been shown to take up to several days to complete their life cycle, thus they may only complete a single round of infection within 72 hours.

To assess this directly in our system, we sought to compare viral infection kinetics among MYXV, vvDD, and MRBV in both adherent and spheroid cultures. Cells were infected with an MOI 10 to maximize infection of all cells at the initial time point. We then assayed cell viability as an initial surrogate to observe virus infection over 5 days. In adherent culture, we found that MRBV was able to induce oncolysis in both HEYA8 and OVCAR8 cells within 24 hours of infection (Figure 3a). In support of our previous findings (Figure 2b), MRBV exhibited a significant delay of infection in adherent SKOV3 cells taking over 48 hours to die from MRBV infection. In contrast, complete oncolysis of adherent EOC cells by MYXV and vvDD required up to 5 days.

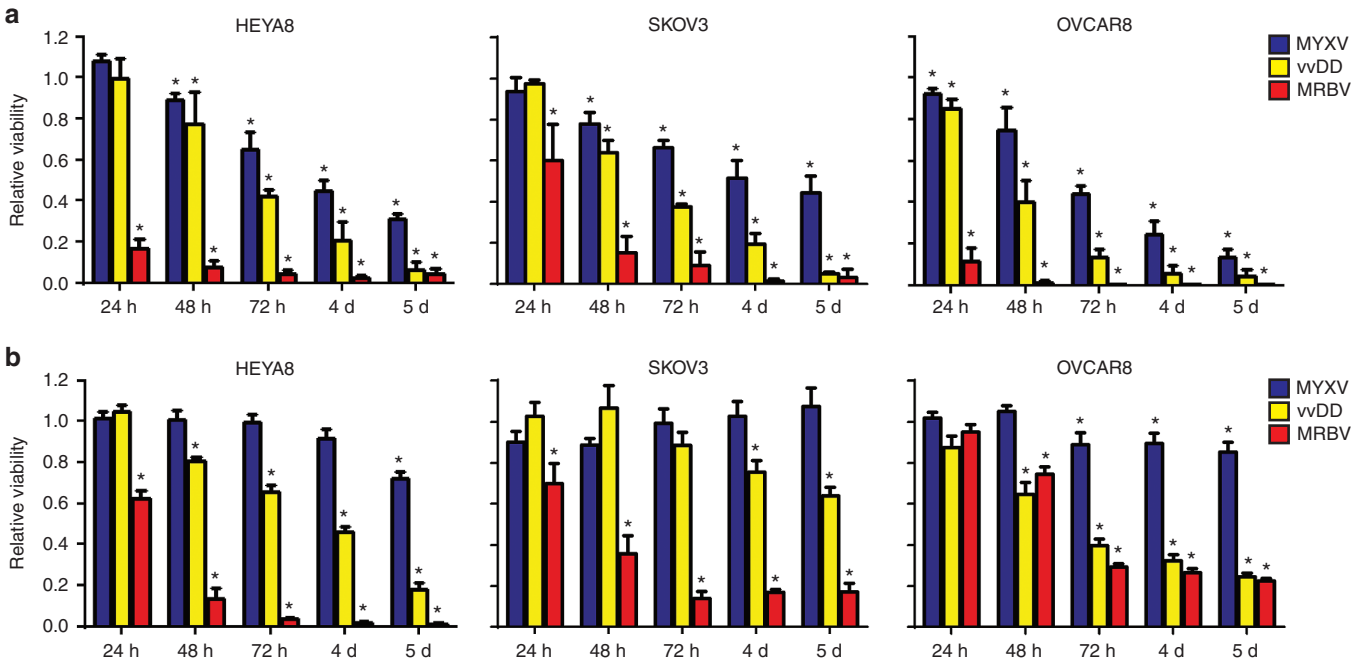

Figure 3 Rapid kinetics of MRBV-mediated killing of epithelial ovarian cancer (EOC) cells and spheroids compared with MYXV and vvDD. (**a**) MRBV-mediated cell killing is observed within 24 hours in adherent EOC cells, but requires longer incubation in SKOV3 cells. Oncolysis of adherent cells by MYXV and vvDD is considerably slower. (**b**) MRBV produces rapid cell killing in spheroids, but there is an incomplete oncolytic effect in SKOV3 and OVCAR8 spheroids. EOC spheroids have reduced viability due to vvDD infection by 5 days, yet remain relatively resistant to MYXV infection (*$P < 0.05$). MYXV, Myxoma virus.

Table 1 Quantification of oncolytic virus production in infected adherent ovarian cancer cells and spheroids

	Adherent culture[a]		
	HEYA8	SKOV3	OVCAR8
MYXV	$1.38 \pm 0.08 \times 10^5$	$5.37 \pm 0.21 \times 10^5$	$1.30 \pm 0.13 \times 10^5$
vvDD	$7.78 \pm 1.22 \times 10^6$	$2.78 \pm 0.35 \times 10^6$	$2.83 \pm 0.59 \times 10^6$
MRBV	$5.52 \pm 1.55 \times 10^7$	$4.82 \pm 1.11 \times 10^7$	$2.38 \pm 0.43 \times 10^7$
	Spheroid culture[b]		
	HEYA8	SKOV3	OVCAR8
MYXV	$8.54 \pm 2.07 \times 10^5$	$1.75 \pm 0.33 \times 10^5$	$1.12 \pm 0.34 \times 10^5$
vvDD	$1.60 \pm 0.21 \times 10^6$	$3.12 \pm 1.58 \times 10^5$	$6.04 \pm 1.39 \times 10^5$
MRBV	$1.09 \pm 0.15 \times 10^8$	$6.80 \pm 0.78 \times 10^6$	$1.58 \pm 0.41 \times 10^6$

[a]In adherent culture, 2.5×10^4 cells were infected in 24-well dishes at MOI 10 (2.5×10^5 pfu). [b]In spheroid culture, 5×10^4 cells were infected in 24-well Ultra-Low Attachment cluster plates at MOI 10 (5×10^5 pfu).
MOI, multiplicity of infection.

We have previously shown that MYXV replication is attenuated in EOC spheroids compared to infection of adherent monolayer cells.[22] Therefore, we tested the kinetics of MYXV, vvDD, and MRBV infection in spheroids to compare directly with our results using proliferating adherent cell lines. We found that MYXV was largely ineffective at inducing detectable oncolysis in EOC spheroids by three days, but cell viability was reduced in HEYA8 and OVCAR8 spheroids by 5 days postinfection (Figure 3b). Although a 72-hour infection of EOC spheroids with vvDD yielded little oncolysis, extending the time course to 5 days was sufficient for marked loss of HEYA8 and OVCAR8 spheroid cell viability. Time course infections with MRBV resulted in cell death between 48 and 72 hours for both HEYA8 and SKOV3 spheroids. Interestingly, OVCAR8 spheroids were relatively resistant to MRBV-mediated cell killing with a limited extent of cell death similar to what we observed for vvDD. This significantly contrasts MRBV infections of adherent EOC cell lines, including OVCAR8 cells, which displayed significant cell death within 24 hours. These unexpected results reinforce the idea that the potential underlying mechanisms governing oncolytic efficacy in EOC cells may be quite dynamic, and stress the importance of preclinical testing in complementary *in vitro* model systems.

MRBV produces significantly more virus progeny than MYXV and vvDD

We postulated that the observed differences in oncolytic effect among the three viruses in our spheroid culture system were also impacted by the efficiency of total virus production. To assess this directly, we infected adherent cells and spheroids and titrated total infectious virus particles. MRBV infection of adherent EOC cell lines yielded significantly more infectious viral progeny compared to both vvDD (7- to 17-fold increase) and MYXV (90- to 400-fold increase) (Table 1). Moreover, the number of viral progeny produced from MRBV infection in adherent culture was relatively similar among the three EOC cell lines. In spheroids, however, infectious progeny produced by MRBV infection was more variable among cell lines. MRBV infection of SKOV3 spheroids yielded 16-fold less virus and OVCAR8 spheroids yielded 69-fold less than HEYA8 spheroids (Table 1). These MRBV titers were congruent with our results of cell viability demonstrating reduced MRBV oncolysis of OVCAR8 spheroids (Figure 2c). The number of viral progeny produced from vvDD infections was similarly reduced in spheroids among cell lines tested. In fact, both MYXV and vvDD were able to produce only a 0.2- to 3.2-fold increase in viral progeny than what was used to initiate infection. Again, this result suggests that EOC spheroids possess physical or molecular changes in cells that significantly impact the replicative life cycle or amplification for both MYXV and vvDD in these dynamic structures.

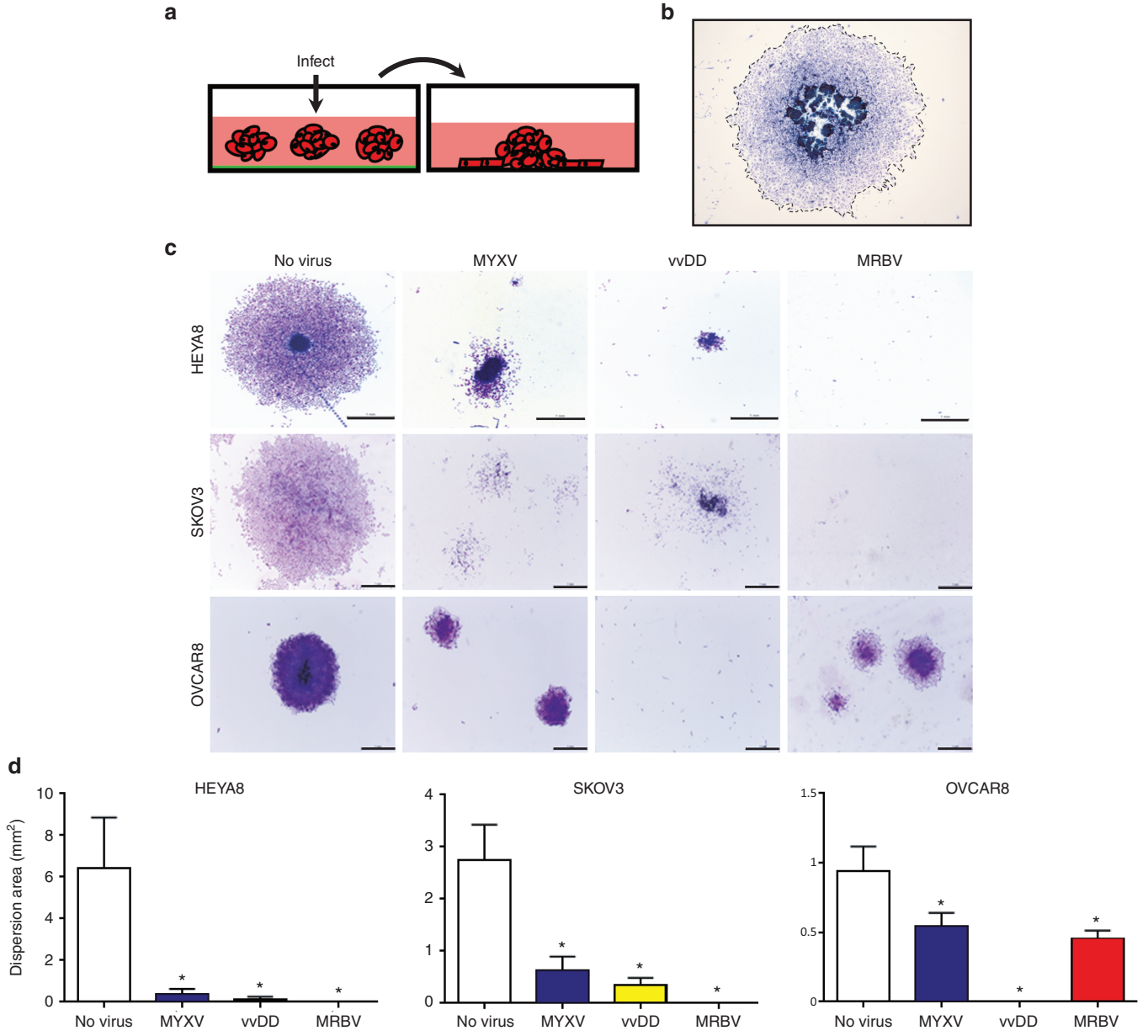

Figure 4 MYXV and vvDD oncolysis is reactivated after spheroid reattachment. (**a**) Schematic representation of spheroid infection followed by reattachment to standard tissue culture-treated plastic. (**b**) Representative image of dispersion area quantification as denoted by dashed outline. (**c**) HEYA8, SKOV3, and OVCAR8 cells were seeded to form spheroids then infected with MYXV, vvDD, or MRBV for 72 hours. Infected spheroids were transferred to adherent culture to allow reattachment for 72 hours, then fixed and stained. Spheroid reattachment was either completely absent (indicating lack of viable cells), or dispersion of cells from the attached spheroid was significantly reduced (indicating reactivation of oncolytic activity upon reattachment to adherent culture). Scale bar: 1 mm. (**d**) Quantification of mean dispersion area was performed using ImageJ software (*$P < 0.05$). MYXV, Myxoma virus.

Activation of MYXV and vvDD oncolysis upon spheroid reattachment

We use spheroid reattachment as a general method to assess cell viability within these structures, as well as to model metastasis formation due to adhesion of spheroids to secondary sites. To this end, EOC spheroids were infected for 72 hours prior to transfer to adherent culture for spheroid reattachment (Figure 4a). Spheroid cells are allowed to reattach and disperse for another 72 hours, after which the dispersion area of cells from infected spheroids was quantified (Figure 4b). Despite lacking a significant oncolytic cell-killing effect in spheroids while in suspension, oncolysis mediated by both MYXV and vvDD was activated upon spheroid reattachment and significantly reduced the ability of cells to disperse from spheroids and form a viable monolayer (Figure 4c,d). Reduced dispersion was apparent within 24 hours after reattachment and sustained for up to 4 days (Supplementary Figure S2). Due to its dramatic impact on spheroid cell viability, MRBV infection completely prevented reattachment of HEYA8 and SKOV3 spheroids (Figure 4c and Supplementary Figure S2). Although our previous results of cell viability indicated a marginal effect of vvDD infection on OVCAR8 spheroids (Figure 2c), vvDD completely prevented OVCAR8 spheroid reattachment suggesting a significant reduction of cell viability in these structures. Interestingly, and in marked contrast to vvDD, MRBV-infected OVCAR8 spheroid cells were still capable of reattaching and dispersing, but to a lesser extent than mock-infected controls (Figure 4c,d and Supplementary Figure S2).

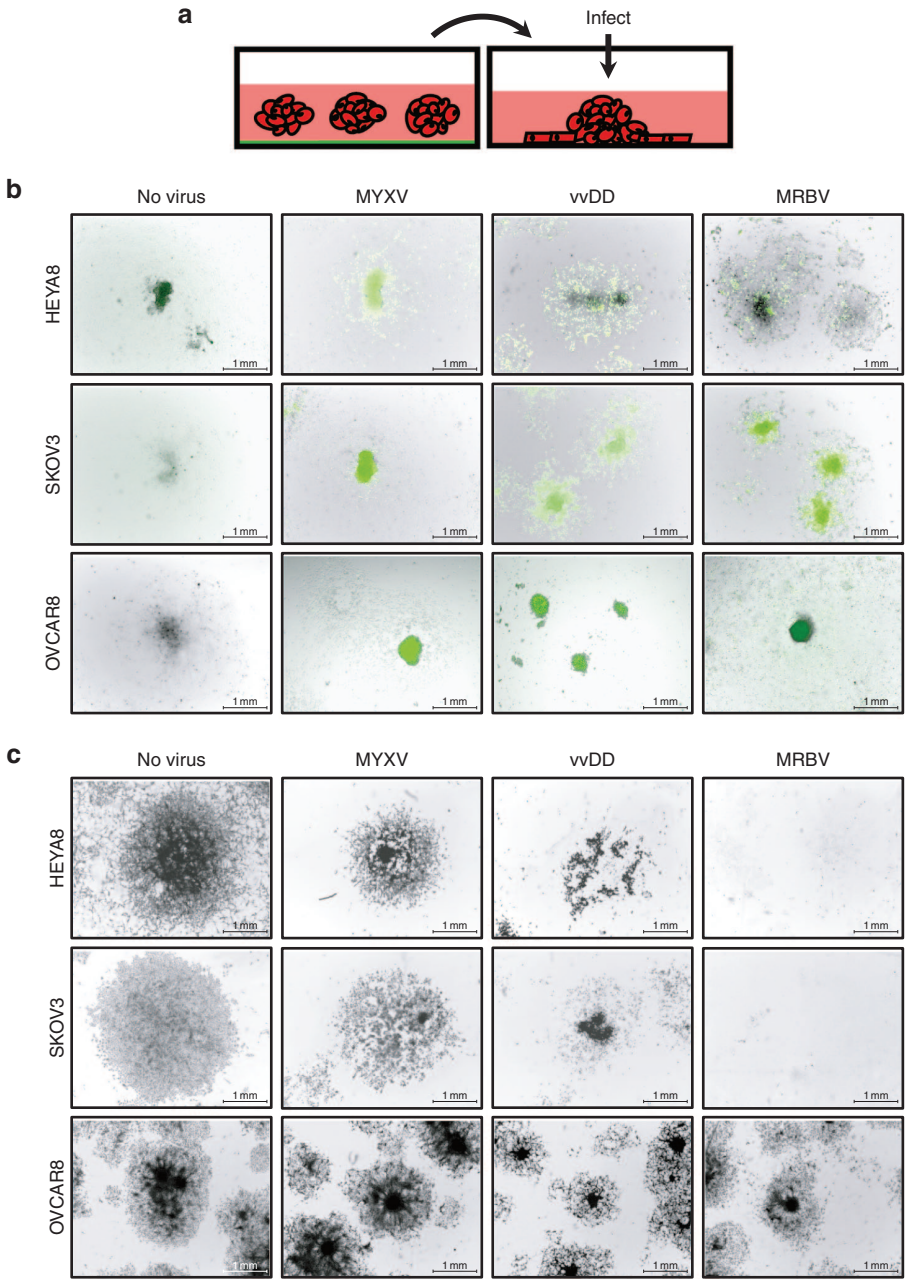

Figure 5 Reattached epithelial ovarian cancer (EOC) spheroids are susceptible to MRBV infection. (**a**) Schematic representation of the infection of reattached spheroids. (**b**) HEYA8, SKOV3, and OVCAR8 cells were seeded to form spheroids, transferred to adherent culture to attach and disperse for 72 hours, and then infected with MYXV, vvDD, or MRBV. Bright field and fluorescence images were captured at 24 hours postinfection and images were merged using Adobe Photoshop software. (**c**) After 72 hours of infection, SKOV3 and HEYA8 spheroids and dispersing cells are completely eradicated by MRBV infection, yet OVCAR8 spheroids and dispersing cells exhibit less oncolytic-mediated cell death. Infection by vvDD is more effective to reduce viable cells than MYXV for all reattached spheroids. Scale bar: 1 mm. MYXV, Myxoma virus.

We next sought to examine the direct oncolytic effect of all three viruses on established reattached spheroids (Figure 5a). This facilitates our ability to evaluate their potential to target metastases, as well as determine whether insensitivity to oncolytic virus infection observed in suspension spheroids also existed in reattached spheroid nodules. We observed virus infection of attached spheroids with treatment of MYXV, vvDD, and MRBV within 24 hours using green fluorescent protein expression as a marker (Figure 5b); this resulted in cytopathic effect in the dispersing adherent cells emanating from attached spheroids while leaving the spheroid cores relatively intact (Figure 5c). These findings further emphasize the requirement of cells to be adherent to promote MYXV- and vvDD-induced oncolysis. Similar to reduced cytopathic efficacy observed in MRBV infection of OVCAR8 spheroids, we observed reduced green fluorescent protein expression in MRBV-infected OVCAR8 attached spheroids when compared with MRBV-infected HEYA8 and SKOV3 attached spheroids, suggesting decreased viral entry or replicative potential in OVCAR8 spheroids.

MRBV entry into EOC spheroid cells is significantly reduced

Since we had observed an appreciable difference for MYXV and vvDD to induce oncolysis of spheroids, and slower infection kinetics of spheroids by MRBV particularly in OVCAR8 spheroids, we sought to determine the efficiency of virus entry into adherent cells and spheroids. To achieve this end, we titrated both the amount of virus remaining in the supernatant and that which had entered the cell. Although we had observed a significant reduction in oncolytic efficacy in EOC spheroids for MYXV and vvDD (Figure 2b,c), there was no significant difference for either MYXV or vvDD to enter adherent or spheroids cells (Figure 6a). In contrast, we observed a significant reduction in the ability of MRBV to enter spheroids for all three EOC cell lines when compared with adherent cells.

Table 2 Summary of overall results for MYXV, vvDD, and MRBV oncolytic efficacy in ovarian cancer adherent cells and spheroids

	HEYA8		*SKOV3*		*OVCAR8*	
	ADH	*SPH*	*ADH*	*SPH*	*ADH*	*SPH*
MYXV	++	–	++	–	++	–
vvDD	++	+	++	–	++	++
MRBV	++++	+++	++++	+++	++++	+

ADH, adherent cells; MYXV, Myxoma virus; SPH, spheroids.

MRBV binding and infection of EOC spheroids requires low-density lipoprotein receptor (LDLR) expression

To investigate the acquired mechanism determining the enhanced ability of MRBV to enter adherent EOC cells compared with spheroids, we postulated this was due to changes in the expression of a cell surface receptor required for MRBV entry. Previous studies have identified the LDLR as a cell surface receptor that is used by the closely-related vesicular stomatitis virus (VSV). Since the glycoprotein responsible for binding and entry of host cells by VSV shares 80% amino acid sequence homology with MRBV glycoprotein, we sought to determine if the mechanism of MRBV entry in EOC cells was LDLR mediated. Indeed, we observed a consistent decrease in the expression of LDLR protein expression in day-3 spheroids when compared with adherent cells among multiple EOC cell lines (Figure 6b). To test this mechanism further, we performed siRNA knockdown of *LDLR* to validate whether LDLR is required by MRBV to gain entry to host cells. *LDLR* knockdown in SKOV3 cells (Figure 6c)

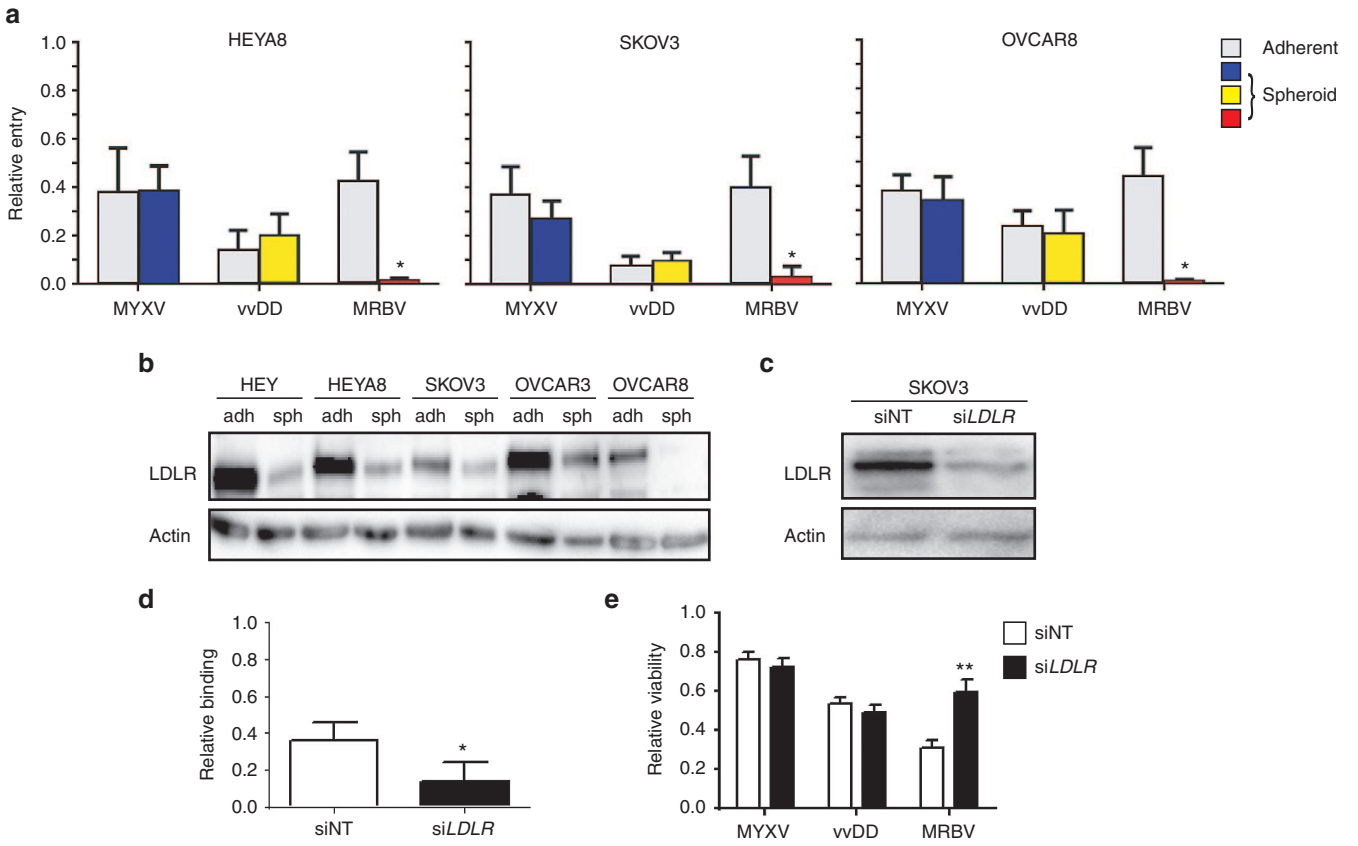

Figure 6 Efficient MRBV entry into ovarian cancer cells requires low-density lipoprotein receptor (LDLR) expression. (**a**) HEYA8, SKOV3, and OVCAR8 cells were seeded to adherent and spheroid culture, and infected with MRBV, vvDD, and MYXV for 1 hour at 4 °C to allow adsorption. Virus titers from cell lysates are shown relative to total virus collected (i.e., supernatant + cells). MRBV titers were determined using supernatant only. Virus treatment in the absence of cells were used as controls. MRBV binding was significantly reduced in EOC spheroids for all three cell lines tested when compared with MYXV and vvDD. (**b**) LDLR protein expression is reduced in ovarian cancer day-3 spheroids as compared with proliferating adherent cells; this results was also observed in the HEY and OVCAR3 cell lines. (**c**) Western blot demonstrating siRNA-mediated LDLR knockdown performed by transient transfection of SKOV3 cells. (**d**) MRBV binding is reduced in SKOV3 cells with *LDLR* knockdown as compared with siNT control transfected cells. (**e**) *LDLR* knockdown significantly decreases MRBV-mediated oncolytic SKOV3 cell death as determined by CellTiter-Glo after 24 hours, whereas there is no effect on viability after MYXV and vvDD infection (*$P < 0.05$; **$P < 0.01$). EOC, epithelial ovarian cancer; MYXV, Myxoma virus.

resulted in a significant decrease in MRBV entry (Figure 6d), and a resultant increase in cell viability in MRBV-infected cells as compared with knockdown control SKOV3 cells (Figure 6e). In contrast, knockdown of *LDLR* had no effect on cell viability due to infection with MYXV or vvDD.

DISCUSSION

Most ovarian cancer patients are diagnosed with late-stage metastatic disease, are subjected to multiple successive recurrences, and will eventually succumb to chemotherapy-resistant disease. Thus, the first objective of this study was to test the potential of MYXV, vvDD, and MRBV as therapeutic alternatives to conventional chemotherapeutics for the treatment of metastatic EOC. A second important objective was to demonstrate that testing viral oncolytics in a uniquely different culture-based model system, *i.e.*, three-dimensional spheroids, can elicit unforeseen results and uncover important mechanisms controlling virus infection and efficacy. MRBV is clearly the most potent oncolytic virus among the EOC cell lines that we tested in both proliferating adherent cells and quiescent 3D spheroids. However, we are the first to discover that endogenous downregulation of LDLR protein expression in spheroids has the potential to reduce MRBV oncolytic efficacy. Although the larger and slower poxviruses MYXV and vvDD were less infectious and produced less virus progeny in ovarian cancer cell lines and spheroids, virus-infected spheroids displayed reduced capacity to reattach and grow due to reactivation of virus infection. Given our results, we propose that early *in vitro* testing of viral oncolytic agents should consider using an experimentally-tractable cell culture system such as ours that mimics unique mechanisms of disease metastasis.

We observed significant differential effects of the three viruses among the three cell lines and when assessing the different steps of metastasis as modeled in our culture system, particularly when comparing adherent to spheroid cells (summarized in Table 2). In adherent culture, MRBV clearly exhibited the highest oncolytic activity. Adherent monolayer cultures represent proliferating ovarian cancer cells with intact growth factor signaling. In contrast, overall efficacy was reduced among the three viruses in spheroids. In particular, the almost universal MRBV oncolytic efficacy was dramatically reduced in OVCAR8 spheroids. We demonstrate that one of the key receptors MRBV utilizes to bind and enter ovarian cancer cells is LDLR; surprisingly, we also show that the LDLR receptor is downregulated in spheroids compared with adherent proliferating ovarian cancer cells. This could be related to the dormant phenotype and the fact that the overall anabolic metabolism is reduced in spheroids.[18,19,23] It has been reported previously that densely-packed cells downregulate LDLR resulting in decreased cholesterol metabolism in gynecologic cancer cell lines.[24,25] It is possible that this same effect of LDLR downregulation is occurring in densely-packed cells comprising EOC spheroids thereby reducing initial virus entry. It is important to note, however, that after this initial delay in virus entry, MRBV is capable of infecting spheroid cells and producing infectious viral progeny albeit with slower kinetics compared with adherent proliferating cells. We postulate that the dormant phenotype observed in cultured spheroids is analogous to microregions of tumors that are avascular or lack essential growth factor and nutrient availability. To that end, it would be important to address LDLR expression level in ovarian tumors directly, and assess whether modifications can be made to increase MRBV binding and entry to the potentially resistant subpopulations due to altered metabolism.

MRBV is the most potent of the three oncolytic viruses tested. It exhibited the greatest killing in the three cell lines. It had the fastest kinetics and generated the most infectious progeny. This is most likely supported by the fact that MRBV is a rhabdovirus with a short life cycle and small genome. This has also been observed for MRBV in other cancer cell systems, and its related family members, such as the most widely-studied rhabdovirus, VSV.[15,26] MRBV was originally identified from a large biorepository of rhabdoviruses as having potent activity in several different cancer cell lines.[15] This group also developed the double point mutant MRBV MG1, which exhibited enhanced growth in cancer cells and reduced effects in normal cells. MRBV is rapidly entering clinical trials with engineered vectors expressing tumor-associated antigens, such as MAGE M3.[27] We postulate that identifying similar tumor-associated antigens specific for ovarian cancer, perhaps other MAGE proteins,[28] could be rapidly applied to develop clinically-useful MRBV oncolytic viral vectors. It has become increasingly evident that oncolytic virus efficacy *in vivo* relies on eliciting an active immune response, which may lead to more durable antitumor effects in the long-term.[29] We recognize that the cell culture-based system used in this report is unable to assess the contribution of the immune system; however, we argue that our *in vitro* ovarian cancer spheroid metastasis model is a useful, rapid and widely-amenable experimental tool for initial testing of novel oncolytic vectors across histologic and molecularly-defined cancer subtypes, particularly using patient-derived malignant tumor cells.

Generally speaking, ovarian cancer spheroids are more restrictive to viral oncolysis. One argument could be made regarding the general physical structure of spheroid that may make them less readily infected by viruses. Interestingly, we found that for MYXV and vvDD viruses there was no difference in binding of these viruses to adherent monolayer cultured cells compared with 3D spheroids in suspension. However, the ability of these two different viruses to complete their lifecycle was dramatically restricted in spheroids. In this case, this is most likely due to the inherent phenotype of ovarian cancer cells in spheroids, namely downregulation of AKT signaling, induction of autophagy, and a cellular quiescent phenotype.[18,19,23] Oncolytic viruses typically rely on overactive or mutant growth factor signaling to promote their life cycle and this constitutes a critical cancer-specific tropism.[30] We have shown in other reports that the AKT signaling pathway is markedly downregulated in ovarian cancer cell spheroids, and this directly affected MYXV oncolytic efficacy.[22] Soares and colleagues have shown that increased levels of phosphorylated AKT are required for late-stage vvDD morphogenesis and production of virus progeny.[31] Likewise, phosphorylated AKT is also required for permissive infection of MYXV; however, the specific stage of the requirement is currently undefined.[32] In our previous study, we demonstrated that activated AKT levels are significantly reduced within spheroids as compared with adherent EOC cells, but this activity is reinstated upon spheroid reattachment.[19] Our present results are in agreement with this phenomenon, since reattachment of spheroids triggered the reactivation of MYXV and vvDD-mediated oncolytic killing of dispersing cells.

MYXV and vvDD reach late-stage virus production in spheroids yet are restricted to cause cell death. This restriction is quickly relieved upon spheroid reattachment when the dormant-to-proliferative switch" occurs[19] and cells are again susceptible to viral-mediated oncolytic cell death. This result is consistent with our previous study using MYXV in patient-derived spheroids.[22] We use spheroid reattachment as a model of intraperitoneal metastatic seeding of malignant cells akin to what is observed in patients.[16,17,33,34] In fact, OVCAR8-generated spheroids were dramatically susceptible to vvDD-induced cell death when using spheroid reattachment as an assay. It would be interesting to determine what mechanisms

are utilized by vvDD to affect OVCAR8 spheroid cells compared with MRBV, an agent that was largely ineffective only in OVCAR8 spheroids. This knowledge may uncover novel strategies to engineer MRBV to make it more widely applicable to ovarian tumors of different histologies and pathobiologies across the ovarian cancer patient spectrum. Given our results, we propose that tumor-homing oncolytic viruses could be potent therapeutic agents with particularly high tropism and efficacy to seek and destroy these persistent microscopic structures in a patient after surgical debulking of macroscopic disease.

MATERIALS AND METHODS

Cell culture

HEYA8, SKOV3, HEY, Vero, HeLa, and BGMK cell lines were cultured in Dulbecco's Modified Eagle medium (Wisent) supplemented with 5% fetal bovine serum (Wisent). OVCAR8 and OVCAR3 cells were cultured in Dulbecco's Modified Eagle medium/F12 (Wisent) containing 10% fetal bovine serum. All cell lines were cultured in a humidified environment at 37 °C with 5% CO_2.

Ascites fluid obtained from ovarian cancer patients at the time of debulking surgery or paracentesis was used to generate primary cell cultures as described previously.[22] Cells were cultured in Dulbecco's Modified Eagle medium/F12 supplemented with 10% fetal bovine serum and grown in a 37 °C humidified atmosphere of 95% air and 5% CO_2. Since these represent primary cell cultures, all experiments were performed between passages 3 and 5. All patient-derived cells were used in accordance with institutional human research ethics board approval (UWO HSREB 12668E).

Virus production

MYXV, vvDD, and MRBV were amplified in BGMK, HeLa, and Vero cell lines, respectively. BGMK cells were infected with MYXV at MOI 10 for 1 hour. After 48 hours of infection, cells were harvested and lysed, cell debris was pelleted by centrifugation and supernatant with MYXV was purified.[35] HeLa cells were infected with vvDD at MOI 0.1 and 60 hours after infection cells and virus were harvested and purified similar to MYXV. Vero cells were infected with MRBV at MOI 0.01. After 20 hours of infection, supernatant was collected and virus was purified using a 0.2 micron filter. All virus constructs have been engineered previously to express green fluorescent protein from endogenous viral promoters: MYXV,[36,37] vvDD,[14] MRBV.[26] The MRBV MG1 mutant strain used in these experiments has been described previously.[26]

Viral titer quantification

Quantification of MYXV, vvDD, and MRBV titers were performed using BGMK, HeLa, and Vero cells, respectively. Virus titers were determined through limiting dilutions of virus on BGMK, HeLa, or Vero. Agarose overlays and plaque assays were performed to determine virus concentration.

Adherent culture. HEYA8, SKOV3, and OVCAR8 cells were seeded at 25,000 cells/well of a 24-well plate and infected with MYXV, vvDD, or MRBV at MOI 10. After 48 hours MRBV infection, and 4 days after MYXV and vvDD infection, cells and supernatant were harvested together for virus content. MYXV, vvDD, and MRBV were titrated on BGMK, HeLa, and Vero cell lines, respectively.

Spheroid culture. HEYA8, SKOV3, and OVCAR8 cells were seeded at 50,000 cells/well of a 24-well Ultra-Low Attachment cluster plate and allowed to form spheroids for 3 days. Spheroids were then infected while in suspension with MYXV, vvDD, or MRBV at MOI 10. Seventy-two hours after MRBV infection, and 5 days after MYXV and vvDD infection, spheroids and supernatant were harvested together for virus content. Spheroids were triturated using a 26-gauge needle and titered as described above.

Virus infection of EOC cells

HEYA8, SKOV3, and OVCAR8 were seeded at 5,000 cells/well of a 96-well plate and were infected the following day with MYXV, vvDD, or MRBV at a MOI 0.001, 0.01, 0.1, 1, and 10. The appropriate UV-inactivated virus at MOI 10 or no virus (mock infected) was used as controls. Seventy-two hours postinfection, viability was assayed using CellTiter-Glo Luminescent Cell Viability Assay (Promega, Madison, WI).

For infection of EOC spheroids, cells were seeded at 50,000 cells/well of a 24-well Ultra-Low Attachment cluster plate (Corning, Corning, NY) and spheroids were allowed to form over 72 hours. Spheroids were then infected at MOI 0.01, 0.1, 1, and 10, using the same controls as described for adherent cell infections.

For infection of reattached spheroids, spheroids were formed as previously described, in the absence of virus, and transferred to six-well tissue culture-treated plates for reattachment. Forty-eight hours after reattachment, spheroids were then infected at MOI 10 based on the initial seeding of 50,000 cells/well of a 24-well Ultra-Low Attachment plate. Spheroids were imaged 24 hours after infection then fixed and stained at 72 hours postinfection using HEMA3 (Fisher HealthCare, Ottawa, Ontario, Canada). Phase contrast and fluorescence images of infected cells and spheroids were captured during each experiment using a Leica DMI 4000B inverted microscope. Fluorescence and phase contrast overlays were generated using Adobe Photoshop.

Kinetics of infection and cell viability

HEYA8, SKOV3, and OVCAR8 cells were seeded as described above for both adherent and spheroid cultures. Cells were then infected with an MOI 10 to allow for maximum virus infection and achieve synchronous virus lifecycle among all cells within the culture. Viability was then assayed using CellTiter-Glo at 12, 24, 36, 48, 72 hours, and 4 and 5 days after infection for adherent cultures and at 24 hours intervals for up to 6 days with spheroids. To assay cell viability in spheroids, spheroids were collected and pelleted, followed by resuspension in CellTiter-Glo and trituration with a 26-gauge needle. Luminescence was measured using a Wallac Plate Reader (PerkinElmer, Waltham, MA).

Spheroid reattachment quantification

Cells were seeded at 50,000 cells/well of a 24-well Ultra-Low Attachment cluster plate to form spheroids over 72 hours. Spheroids were infected with MYXV, vvDD, or MRBV at MOI 10. Spheroids were reattached by transferring to six-well tissue culture plates. Spheroids were permitted to attach and disperse for an additional 72 hours prior to fixing and staining using HEMA3. Dispersion areas were calculated using ImageJ 1.48 software (NIH) by subtracting the area of the core spheroid from the total area of the dispersion zone.

Virus entry quantification

Adherent cells and spheroids were infected with MOI 10 MYXV, vvDD, and MRBV for 1 hour at 4 °C to allow virus infection of cells, but to prevent virus uncoating that would affect subsequent quantification of infectious virus titers. After 1 hour of virus adsorption, supernatant and cells were separated and cell pellets were washed twice with PBS. Spheroids and adherent cells were triturated as described above to ensure that all nonadsorbed virus was released. Virus content from supernatants and cell pellets were titrated separately to quantify the proportion of virus that had entered adherent cells and spheroids.

Immunoblotting

Cell lysates were generated using a modified radioimmunoprecipitation assay (RIPA) buffer (50 mmol/l HEPES pH7.4, 150 mmol/l NaCl, 10% glycerol, 1.5 mmol/l MgCl2, 1 nmol/l ethylene glycol tetraacetic acid, 1 nmol/l sodium orthovanadate, 10 mmol/l sodium pyrophosphate, 10 mmol/l sodium fluoride, 1% Triton X 100, 1% sodium deoxycholate, 0.1% sodium dodecyl sulfate, 1 mmol/l phenylmethylsulfonyl fluoride, 1× protease inhibitor cocktail (Roche, Laval, QC)) as described previously.[38] Lysates were incubated on ice for 20 minutes and vortexed to ensure complete lysis. Lysates from day-3 spheroids were triturated using a 26-gauge needle to help facilitate lysis. Protein concentrations were then determined by Bradford assay using Protein Assay Dye Reagent (BioRad, Mississauga, ON). Thirty micrograms of each lysate were run on an 8% sodium dodecyl sulphate-polyacrylamide gel electrophoresis gel and transferred to a polyvinylidene difluoride membrane (Roche, Mississauga, Ontario, Canada). Blots were blocked with 5% skim milk in Tris-buffered saline with Tween 20 (TBST; 10 mmol/l Tris-HCl, pH 8.0, 150 mmol/l NaCl, 0.1% Tween 20). After 1 hour of blocking, blots were incubated

on a rocking platform shaker at 4 °C overnight with specific antibodies at 1:1,000 dilution in bovine serum albumin (BSA)/TBST (anti-LDLR (Abcam, ab14056; Cambridge, MA); anti-actin (Sigma)). Blots were washed using TBST and incubated with peroxidase-conjugated anti-rabbit IgG (GE Healthcare) at 1:10,000 dilution, 5% skim milk/TBST (LDLR) or 5% bovine serum albumin/TBST (actin), for 1 hour at room temperature. Blots were washed again using TBST followed by incubation with Luminata Forte Western horseradish peroxidase substrate (Millipore, Etobicoke, Ontario, Canada) and visualization of bands with the ChemiDoc MP System (BioRad, Mississauga, Ontario, Canada).

LDL receptor knockdown

SKOV3 cells were seeded in 48-well dishes and transfected the next day with si*LDLR* SMARTPool RNA or the siNT nontargeting control RNA using DharmaFECT 1 transfection reagent (Dharmacon). At 48 hours post-transfection, cells were used for infection experiments (virus entry (MRBV at MOI 0.1) and cell viability (MYXV and vvDD at MOI 1; MRBV at MOI 0.1)) as described above.

Statistical analysis

Statistical significance was determined by unpaired two-tailed Student's *t*-test or one-way analysis of variance using GraphPad Prism 6 (GraphPad Software, San Diego, CA). Statistical significance was set at $P < 0.05$.

CONFLICT OF INTEREST

The authors declared no conflicts of interest.

ACKNOWLEDGMENTS

We acknowledge Milani Sivapragasam, Nicole Lesmeister, and Rachel Dales for assisting with experiments. This work was supported by research grants from the Lawson Internal Research Fund and the London Regional Cancer Program with funds from the London Run for Ovarian Cancer. We are also grateful to the significant funding contributions from the 100 Women Who Care and Plunkett Foundation. JGT was supported by a graduate scholarship from the Strategic Training Program in Cancer Research and Technology Transfer Program with funds from Canadian Institutes of Health Research.

REFERENCES

1. Canadian Cancer Statistics 2014. Public Health Agency of Canada, Ed. pp. 1-132. Government of Canada.
2. The Cancer Genome Atlas Research Network. (2011). Integrated genomic analysis of ovarian carcinoma. *Nature* **474**: 609–615.
3. Howlader, N, Noone, AM, Krapcho, M, Garshell, J, Miller, D, Altekruse, SF *et al.* (2014). SEER Cancer Statistics Review, 1975-2012. National Cancer Institute: Bethesda, MD. http://seer.cancer.gov/csr/1975_2012/.
4. Griffiths, CT (1975). Surgical resection of tumor bulk in the primary treatment of ovarian carcinoma. *Natl Cancer Inst Monogr* **42**: 101–104.
5. Hacker, NF, Berek, JS, Lagasse, LD, Nieberg, RK and Elashoff, RM (1983). Primary cytoreductive surgery for epithelial ovarian cancer. *Obstet Gynecol* **61**: 413–420.
6. Coleman, RL, Monk, BJ, Sood, AK and Herzog, TJ (2013). Latest research and treatment of advanced-stage epithelial ovarian cancer. *Nat Rev Clin Oncol* **10**: 211–224.
7. Ferrandina, G, Fagotti, A, Salerno, MG, Natali, PG, Mottolese, M, Maneschi, F *et al.* (1999). p53 overexpression is associated with cytoreduction and response to chemotherapy in ovarian cancer. *Br J Cancer* **81**: 733–740.
8. Kurman, RJ and Shih, IeM (2010). The origin and pathogenesis of epithelial ovarian cancer: a proposed unifying theory. *Am J Surg Pathol* **34**: 433–443.
9. Tothill, RW, Tinker, AV, George, J, Brown, R, Fox, SB, Lade, S *et al.*; Australian Ovarian Cancer Study Group. (2008). Novel molecular subtypes of serous and endometrioid ovarian cancer linked to clinical outcome. *Clin Cancer Res* **14**: 5198–5208.
10. Kurman, RJ and Shih, IeM (2011). Molecular pathogenesis and extraovarian origin of epithelial ovarian cancer–shifting the paradigm. *Hum Pathol* **42**: 918–931.
11. Russell, SJ, Peng, KW and Bell, JC (2012). Oncolytic virotherapy. *Nat Biotechnol* **30**: 658–670.
12. Kerr, PJ (2012). Myxomatosis in Australia and Europe: a model for emerging infectious diseases. *Antiviral Res* **93**: 387–415.
13. Kim, M, Williamson, CT, Prudhomme, J, Bebb, DG, Riabowol, K, Lee, PW *et al.* (2010). The viral tropism of two distinct oncolytic viruses, reovirus and myxoma virus, is modulated by cellular tumor suppressor gene status. *Oncogene* **29**: 3990–3996.
14. McCart, JA, Ward, JM, Lee, J, Hu, Y, Alexander, HR, Libutti, SK *et al.* (2001). Systemic cancer therapy with a tumor-selective vaccinia virus mutant lacking thymidine kinase and vaccinia growth factor genes. *Cancer Res* **61**: 8751–8757.
15. Brun, J, McManus, D, Lefebvre, C, Hu, K, Falls, T, Atkins, H *et al.* (2010). Identification of genetically modified Maraba virus as an oncolytic rhabdovirus. *Mol Ther* **18**: 1440–1449.
16. Burleson, KM, Casey, RC, Skubitz, KM, Pambuccian, SE, Oegema, TR Jr and Skubitz, AP (2004). Ovarian carcinoma ascites spheroids adhere to extracellular matrix components and mesothelial cell monolayers. *Gynecol Oncol* **93**: 170–181.
17. Burleson, KM, Hansen, LK and Skubitz, AP (2004). Ovarian carcinoma spheroids disaggregate on type I collagen and invade live human mesothelial cell monolayers. *Clin Exp Metastasis* **21**: 685–697.
18. Lu, Z, Luo, RZ, Lu, Y, Zhang, X, Yu, Q, Khare, S *et al.* (2008). The tumor suppressor gene ARHI regulates autophagy and tumor dormancy in human ovarian cancer cells. *J Clin Invest* **118**: 3917–3929.
19. Correa, RJ, Peart, T, Valdes, YR, DiMattia, GE and Shepherd, TG (2012). Modulation of AKT activity is associated with reversible dormancy in ascites-derived epithelial ovarian cancer spheroids. *Carcinogenesis* **33**: 49–58.
20. Makhija, S, Taylor, DD, Gibb, RK and Gerçel-Taylor, C (1999). Taxol-induced bcl-2 phosphorylation in ovarian cancer cell monolayer and spheroids. *Int J Oncol* **14**: 515–521.
21. Domcke, S, Sinha, R, Levine, DA, Sander, C and Schultz, N (2013). Evaluating cell lines as tumour models by comparison of genomic profiles. *Nat Commun* **4**: 2126.
22. Correa, RJ, Komar, M, Tong, JG, Sivapragasam, M, Rahman, MM, McFadden, G *et al.* (2012). Myxoma virus-mediated oncolysis of ascites-derived human ovarian cancer cells and spheroids is impacted by differential AKT activity. *Gynecol Oncol* **125**: 441–450.
23. Liao, J, Qian, F, Tchabo, N, Mhawech-Fauceglia, P, Beck, A, Qian, Z *et al.* (2014). Ovarian cancer spheroid cells with stem cell-like properties contribute to tumor generation, metastasis and chemotherapy resistance through hypoxia-resistant metabolism. *PLoS ONE* **9**: e84941.
24. Kruth, HS, Avigan, J, Gamble, W and Vaughan, M (1979). Effect of cell density on binding and uptake of low density lipoprotein by human fibroblasts. *J Cell Biol* **83**: 588–594.
25. Gal, D, MacDonald, PC, Porter, JC, Smith, JW and Simpson, ER (1981). Effect of cell density and confluency on cholesterol metabolism in cancer cells in monolayer culture. *Cancer Res* **41**: 473–477.
26. Stojdl, DF, Lichty, B, Knowles, S, Marius, R, Atkins, H, Sonenberg, N *et al.* (2000). Exploiting tumor-specific defects in the interferon pathway with a previously unknown oncolytic virus. *Nat Med* **6**: 821–825.
27. NCIC Clinical Trials Group (2014). MG1 Maraba/MAGE-A3, With and Without Adenovirus Vaccine, With Transgenic MAGE-A3 Insertion in Patients With Incurable MAGE-A3-Expressing Solid Tumours. National Library of Medicine (US): Bethesda, MD.
28. Daudi, S, Eng, KH, Mhawech-Fauceglia, P, Morrison, C, Miliotto, A, Beck, A *et al.* (2014). Expression and immune responses to MAGE antigens predict survival in epithelial ovarian cancer. *PLoS ONE* **9**: e104099.
29. Lichty, BD, Breitbach, CJ, Stojdl, DF and Bell, JC (2014). Going viral with cancer immunotherapy. *Nat Rev Cancer* **14**: 559–567.
30. Chiocca, EA (2002). Oncolytic viruses. *Nat Rev Cancer* **2**: 938–950.
31. Soares, JA, Leite, FG, Andrade, LG, Torres, AA, De Sousa, LP, Barcelos, LS *et al.* (2009). Activation of the PI3K/Akt pathway early during vaccinia and cowpox virus infections is required for both host survival and viral replication. *J Virol* **83**: 6883–6899.
32. Werden, SJ and McFadden, G (2010). Pharmacological manipulation of the akt signaling pathway regulates myxoma virus replication and tropism in human cancer cells. *J Virol* **84**: 3287–3302.
33. Shield, K, Ackland, ML, Ahmed, N and Rice, GE (2009). Multicellular spheroids in ovarian cancer metastases: Biology and pathology. *Gynecol Oncol* **113**: 143–148.
34. Burleson, KM, Boente, MP, Pambuccian, SE and Skubitz, AP (2006). Disaggregation and invasion of ovarian carcinoma ascites spheroids. *J Transl Med* **4**: 6.
35. Smallwood, SE, Rahman, MM, Smith, DW and McFadden, G (2010). Myxoma virus: propagation, purification, quantification, and storage. *Curr Protoc Microbiol* **Chapter 14**: Unit 14A.1.
36. Opgenorth, A, Graham, K, Nation, N, Strayer, D and McFadden, G (1992). Deletion analysis of two tandemly arranged virulence genes in myxoma virus, M11L and myxoma growth factor. *J Virol* **66**: 4720–4731.
37. Johnston, JB, Barrett, JW, Chang, W, Chung, CS, Zeng, W, Masters, J *et al.* (2003). Role of the serine-threonine kinase PAK-1 in myxoma virus replication. *J Virol* **77**: 5877–5888.
38. Shepherd, TG, Mujoomdar, ML and Nachtigal, MW (2010). Constitutive activation of BMP signalling abrogates experimental metastasis of OVCA429 cells via reduced cell adhesion. *J Ovarian Res* **3**: 5.

Supplementary Information accompanies this paper on the *Molecular Therapy—Oncolytics* website (http://www.nature.com/mto)